PROCEEDINGS OF SCIENCE

Medium effects on hadrons and jets in $\sqrt{s_{\mathrm{NN}}} = 200$ GeV isobar collisions at STAR

Tristan Protzman[a,*] **on behalf of the STAR collaboration**

[a] *Lehigh University, Bethlehem, PA*

E-mail: tlp220@lehigh.edu

Partonic scatterings with large momentum transfer occur before the formation of the quark-gluon plasma (QGP) in heavy-ion collisions, resulting in collimated collections of hadrons known as jets. As a jet traverses and interacts with the QGP medium, it loses energy via collisional and radiative processes, known as jet quenching. The path-length dependence of jet quenching processes can be studied by measuring the azimuthal anisotropy of jet yields relative to the event plane, quantified by the second-order Fourier coefficient v_2. A finite jet v_2 is expected in mid-central heavy-ion collisions where a highly ellipsoidal QGP medium is formed, resulting in jets traversing in-plane interacting with less medium than those out-of-plane. In these proceedings, we report measurements of charged jet v_2 in isobar collisions spanning multiple jet resolutions. Ongoing work to use event shape engineering to more precisely control the path length of the initiating partons will also be discussed.

26-31 March 2023
Aschaffenburg, Germany

[*] Speaker

1. Introduction

To better understand the kinematics of partons traveling through the quark-gluon plasma (QGP) produced in heavy-ion collisions, it is useful to identify a well understood probe which experiences the medium. Jets are one such probe, which are collimated sprays of particles initiated from a hard (high-Q^2) partonic scattering. Due to their early formation time, jets experience the full evolution of the QGP. In particular, the phenomenon of jet quenching, where a jet loses energy through collisional and radiative QCD processes while traversing the QGP, can yield insight into QGP dynamics.

The jet energy loss and subsequent yield suppression are measured with the nuclear modification factor, $R_{\rm AA}$, where a value less than one is interpreted as a suppression of the yield in A+A collisions relative to p+p collisions. However, this observable is integrated over all possible paths. Path-length differences can be treated on an ensemble level by quantifying the yield differentially with respect to the event plane.

In a semi-central heavy-ion collision, the produced QGP is approximately elliptical in geometry. As a result, jets that are produced parallel to the second order event plane will experience a shorter mean path length than those which are produced transverse to it. This can be quantified with the second-order Fourier coefficient v_2, defined as

$$\frac{dN}{d\Delta\phi} \propto 1 + 2v_2 \cos 2\Delta\phi. \tag{1}$$

A positive v_2 indicates a greater suppression of the yield out-of-plane relative to in-plane, and thus can be interpreted as an indication of path-length dependent jet quenching. Presented in these proceedings are measurements of charged jet v_2 carried out by the STAR Collaboration in $\sqrt{s_{\rm NN}}$ = 200 GeV Ru+Ru and Zr+Zr collisions.

2. Analysis methods

In this analysis, data from the 2018 isobar collisions is analyzed, consisting of Ru+Ru and Zr+Zr collisions, with each species containing 96 nucleons. A subset of the STAR detector's subsystems is utilized, including the Time Projection Chamber (TPC) [1], the Barrel Electromagnetic Calorimeter (BEMC) [2], and the Event Plane Detector (EPD) [3].

To select jet-like events, events in which at least 3.4 GeV is deposited in one tower of the BEMC are analyzed. The reconstructed primary vertex is required to satisfy $-35 < v_z < 25$ cm along the beam axis and $v_r < 2$ cm radially from the nominal beam center. An additional requirement of $|v_z - v_{z,\rm vpd}| < 5$ cm is used to reject events with pileup, where $v_{z,\rm vpd}$ is reconstructed with the Vertex Position Detector [4].

Charged particle tracks in the TPC are required to be reconstructed with a minimum of 15 spatial points and at least 52% of possible points. Additionally, their momenta must satisfy $0.2 < p_{\rm T} < 30$ GeV/c and they must project to within 1 cm of the primary vertex. The multiplicity in the TPC in the region $|\eta| < 0.5$ is used to select events in the 20-60% centrality region.

2.1 Event plane determination

The event plane is measured at forward rapidity using the EPD, a segmented scintillating detector covering $2.1 < \eta < 5.1$. A two-step flattening procedure is applied as described in [5]. First, for each of the 16 rings of the EPD a tile-by-tile weight is determined such that the average signal within a given ring is normalized. Next, an event-by-event shift to the measured event plane, $\Delta\Psi_2$, is determined such that the overall event plane distribution is isotropic.

The event plane resolution is determined using the sub-event method, comparing the event plane as measured by the East and West EPD.

$$R(\Psi_2) = \sqrt{2\,\langle \cos 2(\Psi_{\mathrm{East}} - \Psi_{\mathrm{West}})\rangle}. \tag{2}$$

In the centrality range 20-60%, the measured event plane resolution is 33.5%.

2.2 Jet finding

Charged particle jets are identified with the anti-k_{T} algorithm [6, 7] using tracks found in the TPC. Resolution parameters of $R = 0.2$, 0.4, and 0.6 are used. A fiducial cut of $|\eta_{\mathrm{jet}}| < 1 - R$ is applied. To correct for the fluctuating background in a heavy-ion environment, the median background momentum density ρ is estimated event-by-event using k_{T} jets with the same resolution parameter, excluding the two hardest jets. The median background is then modulated relative to the event plane by an average $v_2 = 0.04$, as measured in Ref. [8]. An event-by-event determination of the underlying background anisotropy results in greater systematic uncertainty than an ensemble level treatment. The raw jet transverse momentum $p_{\mathrm{T}}^{\mathrm{raw}}$ is corrected by

$$p_{\mathrm{T}}^{\mathrm{reco}} = p_{\mathrm{T}}^{\mathrm{raw}} - A\rho(\Delta\phi), \tag{3}$$

where A is the jet area determined by embedding ghost particles into the event [9], and $\Delta\phi$ is the angle between the jet and the event plane.

This population of jets still contains a large combinatorial contribution, which are jets clustered from fluctuations in the event background. To remove these jets, a hard-core matching routine is utilized [10]. This is done by clustering tracks with $p_{\mathrm{T}} > 2$ GeV/c with the anti-k_{T} algorithm and the same jet resolution parameter. Jets are matched to hard cores with $p_{\mathrm{T}} > 10$ GeV/c geometrically, and only jets that are within $\Delta R < R$ are accepted, where

$$\Delta R = \sqrt{\left(\eta_{\mathrm{jet}} - \eta_{\mathrm{hard\ core}}\right)^2 + \left(\phi_{\mathrm{jet}} - \phi_{\mathrm{hard\ core}}\right)^2} \tag{4}$$

is the distance between the jet axis $\left(\eta_{\mathrm{jet}},\ \phi_{\mathrm{jet}}\right)$ and the hard core axis $(\eta_{\mathrm{hard\ core}},\ \phi_{\mathrm{hard\ core}})$. This effectively requires the jet ensemble to have a hard fragmentation pattern, potentially introducing a bias on the selected jet population.

2.3 Determination of azimuthal anisotropy

To determine the azimuthal anisotropy, jet yields are measured as a function of $p_{\mathrm{T}}^{\mathrm{reco}}$ and $\Delta\phi$, where $\Delta\phi$ is the azimuthal distance between the jet and the event plane in the domain $0 \leq \Delta\phi \leq \pi/2$. For each $p_{\mathrm{T}}^{\mathrm{reco}}$ bin, v_2^{obs} is determined by fitting the data with Eq. 1, with the statistical uncertainty

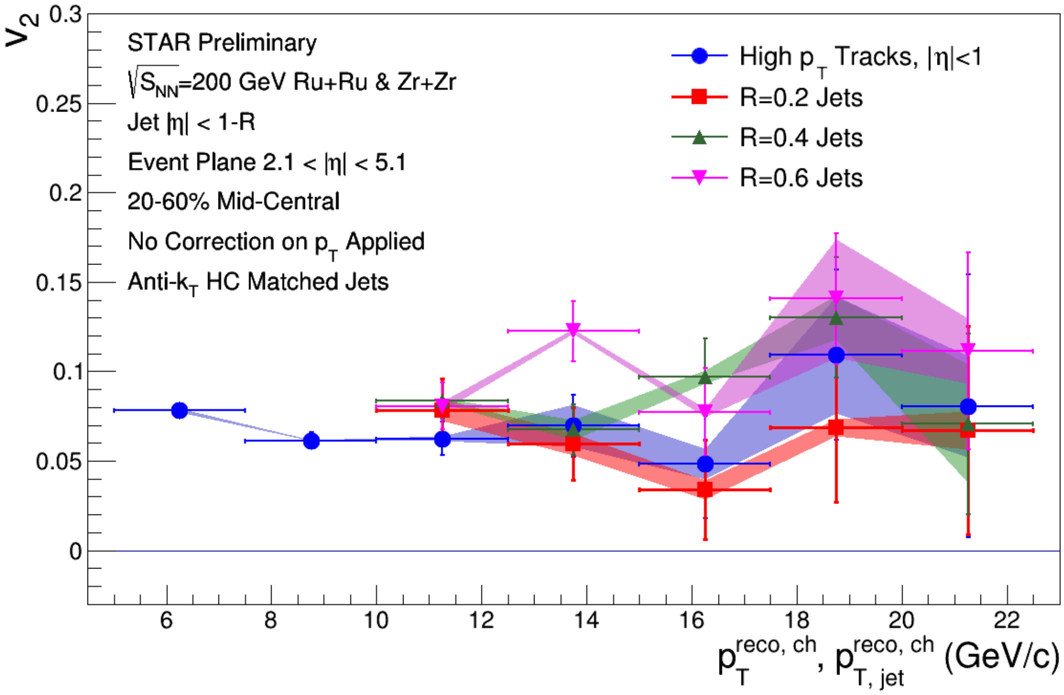

Figure 1: Jet v_2 for high-p_T tracks (blue) and $R = 0.2$ (red), 0.4 (green), and 0.6 (magenta) anti-k_T jet resolutions. Across all resolutions, no strong dependence on the transverse momentum is observed.

determined by the uncertainty of the fit. The true v_2 is reached by correcting the observed v_2^{obs} with the event plane resolution,

$$v_2 = \frac{v_2^{obs}}{R(\Psi_2)}. \tag{5}$$

The dominant sources of systematic uncertainties are from the tracking efficiency of the TPC and in the estimation of a mean background v_2 of 0.04. To account for these, the analysis was repeated randomly removing 4% of tracks in addition to thse lost due to detector inefficiency to understand the dependence on the tracking efficiency and varying the assumed background v_2 to 0.02 and 0.06 to determine the sensitivity to the background.

3. Results

Jet v_2 is presented for charged particles with $5 < p_T < 22.5$ GeV/c and for charged jets with $10 < p_T^{reco} < 22.5$ GeV/c for $R = 0.2$, 0.4, and 0.6 in Fig. 1. No strong transverse momentum dependence is observed. In the overlapping kinematic region, the measured v_2 is consistent with that of the ALICE measurement in $\sqrt{s_{NN}} = 2.76$ TeV Pb+Pb collisions [11].

To quantify the jet v_2 dependence on the jet resolution parameter, the ratio of $R = 0.4$ and $R = 0.6$ to $R = 0.2$ charged jet v_2 is measured, integrated from $10 < p_T^{reco} < 22.5$ GeV/c since no transverse momentum dependence was observed. This is shown in Fig. 2. To avoid an autocorrelation arising from comparing populations containing some of the same jets, the dataset

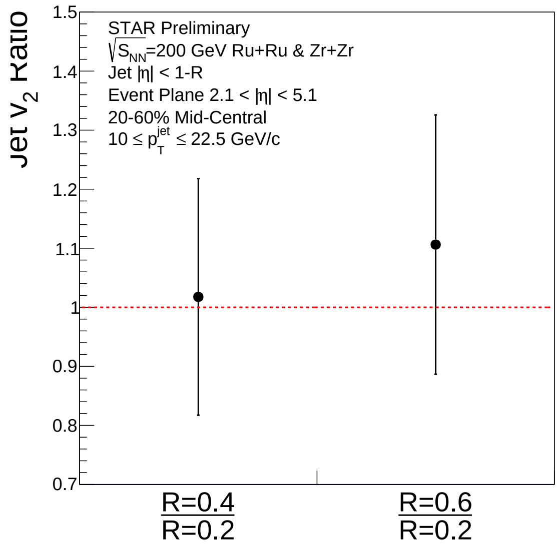

Figure 2: The charged jet v_2 ratio of larger jet resolutions to $R = 0.2$ anti-$k_{\rm T}$ jets. To avoid autocorrelations, the data is divided into two parts used separately for the numerator and denominator. Within uncertainties, no dependence on the jet resolution is observed.

is divided into two statistically independent sets for the numerator and denominator. Within the available uncertainties, no dependence on the jet resolution parameter is observed.

4. Conclusions

A non-zero jet v_2 observed in heavy-ion collisions may be interpreted as an indication of path-length dependent jet quenching. However, it is important to consider a potential geometric bias imposed on the jet population, selecting jets that preferentially are formed near the surface of the QGP due to the hard core selection criteria. For a more complete interpretation of jet v_2, data-model comparisons should be made for v_2 as well as $R_{\rm AA}$.

Further complicating the interpretation of a positive jet v_2 solely as path-length dependent quenching is the presence of jet v_2 in small p+A systems which lack other quenching signatures [12]. By measuring jet v_2 in a medium-sized system with 96 nucleons, the aim of this work is to inform our understanding the transition between the dominant processes in Au+Au and Pb+Pb systems and small p+A systems.

Ongoing work to this goal includes utilizing event-shape engineering (ESE) to further constrain the path length, as well as measuring jet v_2 in more intermediate systems. Using ESE, events within a given centrality class are further divided into eccentricity classes, controlling the energy density while varying the event shape [13].

References

[1] M. Anderson et al., *The Star time projection chamber: A Unique tool for studying high multiplicity events at RHIC*, *Nucl. Instrum. Meth. A* **499** (2003) 659 [nucl-ex/0301015].

[2] STAR collaboration, *The STAR barrel electromagnetic calorimeter*, *Nucl. Instrum. Meth. A* **499** (2003) 725.

[3] J. Adams et al., *The STAR Event Plane Detector*, *Nucl. Instrum. Meth. A* **968** (2020) 163970 [1912.05243].

[4] W.J. Llope et al., *The STAR Vertex Position Detector*, *Nucl. Instrum. Meth. A* **759** (2014) 23 [1403.6855].

[5] A.M. Poskanzer and S.A. Voloshin, *Methods for analyzing anisotropic flow in relativistic nuclear collisions*, *Phys. Rev. C* **58** (1998) 1671 [nucl-ex/9805001].

[6] M. Cacciari, G.P. Salam and G. Soyez, *The anti-k_t jet clustering algorithm*, *JHEP* **04** (2008) 063 [0802.1189].

[7] M. Cacciari, G.P. Salam and G. Soyez, *FastJet User Manual*, *Eur. Phys. J. C* **72** (2012) 1896 [1111.6097].

[8] STAR collaboration, *Search for the chiral magnetic effect with isobar collisions at* $\sqrt{s_{NN}}$*=200 GeV by the STAR Collaboration at the BNL Relativistic Heavy Ion Collider*, *Phys. Rev. C* **105** (2022) 014901 [2109.00131].

[9] M. Cacciari and G.P. Salam, *Pileup subtraction using jet areas*, *Phys. Lett. B* **659** (2008) 119 [0707.1378].

[10] STAR collaboration, *Dijet imbalance measurements in Au + Au and* pp *collisions at* $\sqrt{s_{NN}}$ = 200 *GeV at STAR*, *Phys. Rev. Lett.* **119** (2017) 062301 [1609.03878].

[11] ALICE collaboration, *Azimuthal anisotropy of charged jet production in* $\sqrt{s_{\rm NN}}$ *= 2.76 TeV Pb–Pb collisions*, *Nucl. Phys. A* **956** (2016) 629 [1511.05352].

[12] ATLAS collaboration, *Transverse momentum and process dependent azimuthal anisotropies in* $\sqrt{s_{\rm NN}}$ = 8.16 *TeV p+Pb collisions with the ATLAS detector*, *Eur. Phys. J. C* **80** (2020) 73 [1910.13978].

[13] P. Christiansen, *Event-Shape Engineering and Jet Quenching*, *J. Phys. Conf. Ser.* **736** (2016) 012023 [1606.07963].